# Effect of beaming and enhanced transmission in photonic crystals

R. Moussa,[1] B. Wang,[1] G. Tuttle,[2] Th. Koschny,[1,3] and C. M. Soukoulis[1,3]

[1]*Ames Laboratory and Department of Physics and Astronomy, Iowa State University, Ames, Iowa 50011, USA*

[2]*Department of Electrical and Computer Engineering and Microelectronics Research Center, Iowa State University, Ames, Iowa 50011, USA*

[3]*Institute of Electronic Structure and Laser, FORTH, and Department of Materials Science and Technology, University of Crete, 71110, Heraklion, Crete, Greece*

The effect of the modified surface and grating layers on the beaming of the electromagnetic waves from a two dimensional photonic crystal (PC) is presented numerically and experimentally. The role of the two components of the beaming, the transmission of the channel and the directionality, are explicitly analyzed. It is demonstrated that a small change, which consists of taking away one grating from the grating layers, can improve the beaming by 20% and opens up a new window of frequencies with a second beaming in our PC. These experimental observations can be explained by the derived dispersion relation of the surface waves. An animated result concludes this study and recapitulates all the observed effects.

In 1998, Ebbesen *et al.*[1] observed an extraordinary optical transmission through subwavelength hole arrays in optically opaque metal films. It has been shown that this enhancement of transmission is due to the excitation of surface plasmons on the metal-dielectric interfaces.[2] Later on, several experimental works[3,4] have shown the possibility of enhancing and channeling a beam through metallic structures. The key feature was to corrugate the surface surrounding the aperture, allowing the excited surface plasmons at the metallic interface to couple to the outgoing beam (propagating modes), leading to a well directed beam. The potential of applications of such kind of structures has been mentioned in several publications.[5–7] Similarly, photonic crystals (PCs) have been shown to support surface waves[8–11] if their operational frequency is within the photonic band gap. In contrast to metallic surfaces that easily excite surface modes, PCs do not support surface waves unless they are appropriately terminated. In this case, surface termination means that the unit cells of the periodic PC located at the surfaces of the PC are chosen to be different from the bulk unit cells. Surface waves in PCs are also excited if the geometry (radius or shape) of the cylinders or bars forming the first and/or last layer of the PC are different from those forming the bulk.[12] This technique is simple and easily handled experimentally. Throughout this paper, the layer with the modified geometrical parameters will be called the modified surface layer. Since the frequency of the incident beam is within the photonic band gap of the PC, the PC will behave as a mirror prohibiting any beam from propagating inside. In order to allow the propagation inside the PC, a line defect is introduced leading to a waveguide mode. This waveguide or channel is nothing but a localized disturbance that breaks the translational symmetry at the interface. Consequently, it couples different wave vector components and allows an incoming normally incident propagating wave with a wave vector $k_\parallel = 0$ to couple to the surface modes with $k_\parallel > \frac{\omega}{c}$, where $\omega$ is the frequency and $c$ is the vacuum speed of light. Several waveguide structures based on PC have been proposed.[13–16] Qualitative[17] and quantitative[18,19] explanations of the physics behind the phenomena have been reported. However, the problem of a poor coupling between the incident wave and the waveguide which is not specific to the PC structures, leads to a low transmission efficiency. This problem is solved by choosing the right modified surface layer that allows surface modes to grow on the surfaces. These two PC features, i.e., supporting surface waves as well as prohibiting the propagation of the electromagnetic (EM) wave inside the PC, except in the waveguide, make them a better substitute to metallic structures. Indeed, the Ohmic losses in metallic structures limit their performance in exciting surface plasmons, the key feature for the enhanced transmission and the high directionality of the beam. Once the surface waves are excited, the next step is to induce the EM waves at the surface to radiate their energy into propagating waves just a few degrees wide. This task is achieved by adding a grating layer at the top of the modified surface layer (the way the modified surface and grating layers are designed and added will be discussed later on). Under specific conditions, the grating layer destructively interferes with the waves everywhere, except about the axis of the waveguide, resulting to a beaming of the propagating modes in the forward direction. Since a better performance of the beaming involves a good transmission of the waveguide together with a better directionality, it is important to be able to track this performance based on a good knowledge of what is the percentage of the beaming coming from the transmission in the channel and what is coming from the directionality. To our knowledge, this issue has not been addressed in earlier papers studying the beaming in PC structures.[13–16] Most recently, Bauer and John[20] demonstrated directional emission from a PC waveguide using the diffraction from scatters at the immediate surrounding of the channel aperture. In contrast to our result discussed in this paper, the latter mechanism described in the paper of Bauer and John apparently does not depend on the excitation of surface modes on the PC to air interface or their dispersion.

The transmission of the channel is very sensitive to the width, length, and essentially the termination of the channel. Once again, by termination or end of the channel, we mean what is exactly at the end of the channel. It could be one rod
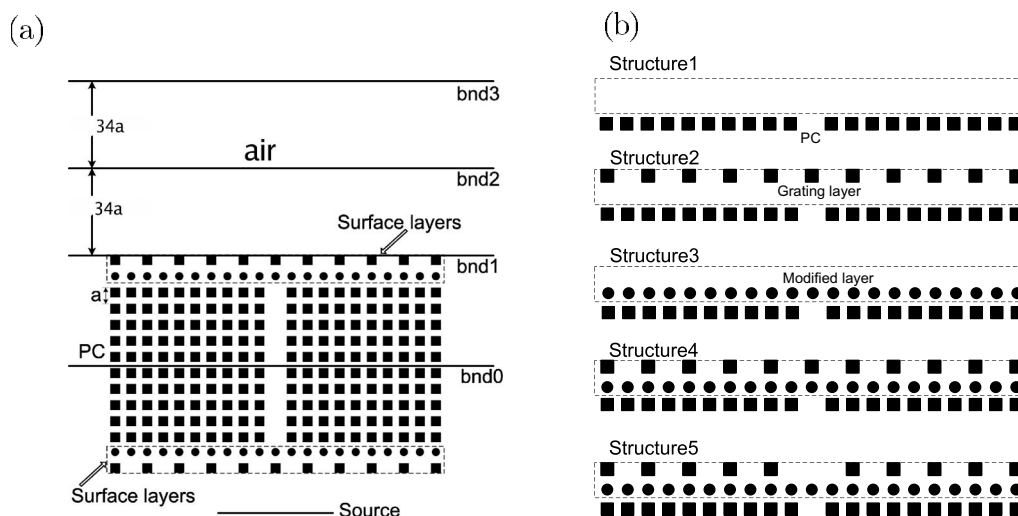
FIG. 1. (a) The structure's details and definition of the different boundaries used. bnd0, bnd1, bnd2, and bnd3 are the boundaries in the channel, at the end of the PC, in the middle of the air part and at the end of the air part respectively. (b) The shape of the surface layers in each of the five different structures.

of the modified surface layer or one rod of the grating layer or one at the top of the other one or simply nothing. The ends or termination of the channel determines basically the back and forth reflection and the Fabry-Perot effects taking place inside the channel. Any changes in the modified surface or the grating layers will affect the excited surface modes as well as the termination of the channel, leading to a change in the transmission of the channel. Even though a few papers have already tried to explain the physics behind the beaming in the PCs,[17–19] we believe that the new physics in this paper reside in the main understanding of the two components of a good beaming, which includes a high channel transmission together with a very good directionality. We succeeded in this paper in separating the two effects and studying them separately. Second, since the key feature of the good beaming is the excitation of the surface waves and this enables them to couple to the outgoing beam, this study allow us, despite the limited size of the structure and with the knowledge of the dispersion of the system, to predict which conditions lead to higher excited surface waves and, consequently, to a better beaming. Therefore, it is important to study the effect of the modified surface and the grating arrays added to the PC on the surface waves and their coupling to the outgoing modes.

The PC examined in this paper consists of a two dimensional square array of dielectric square bars with a dielectric constant $\varepsilon = 9.8$ in air. The dimensions of the structure are 21 layers in the lateral direction and 10 layers in the propagation direction with a lattice constant $a = 11$ mm. The width of each square dielectric bar is 3.18 mm. A schematic picture of the PC structure and the arrangement for both experiments and simulations are shown in Fig. 1. In order to create a waveguide, we omit the ten bars forming the middle row in the structure to channel the beam through it. The actual aperture's width of the waveguide is approximately 1.9 cm, measured from the outer-part bars of the PC. Therefore, for all the frequencies of the incident plane wave (between 10 and 13 GHz), the aperture is smaller than the wavelength of

the incident beam. Consequently, we expect the aperture to transmit very poorly and diffract light in all directions. For the modified surface layer, we add a row of circular rods of radius of 0.915 mm at the beginning and the end of the PC. As a grating layer, a row of square rods of width of 3.18 mm is added to the structure with a lattice constant twice the lattice constant of the PC (see Fig. 1). A finite plane wave source with width of 7.85 cm is placed at a distance 3 cm from the outer interface of the structure. The commercial finite element method software FEMLAB (COMSOL) was used to calculate the field distribution of the different structures under study.[21] In all the simulations we performed, perfect matched layer[22] boundary conditions were used to surround the computational domain. For both experimental and numerical results, a TM polarization (the electric field E is parallel to the axis of the rods) is used. Transmission measurements were performed to verify and test the enhancement as well as the beaming. The experimental setup consists of an HP 8510C network analyzer, a horn antenna as the transmitter, and a monopole antenna as the receiver.

The photonic band gap of the PC is situated between 8.8 and 12.80 GHz. To differentiate between the portion of the beaming coming from the transmission of the channel and the one coming from the directionality, the following forms of structures have been studied: the waveguide by itself is referred to as structure 1, the waveguide with the grating layers is referred to as structure 2, the waveguide with the modified surface layers is referred to as structure 3, and the waveguide with both the modified surface and grating layers is referred to as structure 4 [see Fig. 1(b)]. The power flow, which is the time average of the poynting vector integrated along the appropriate boundary, for each of these structures is examined in different boundaries in the propagation direction, as shown in Fig. 1(a). The first, second, and third boundaries located at the end of the PC, the middle of the air part, and the end of the air part are referred to as bnd1, bnd2, and bnd3, respectively. The boundary bnd0, located in the middle of the PC, is the boundary used for normalization. It
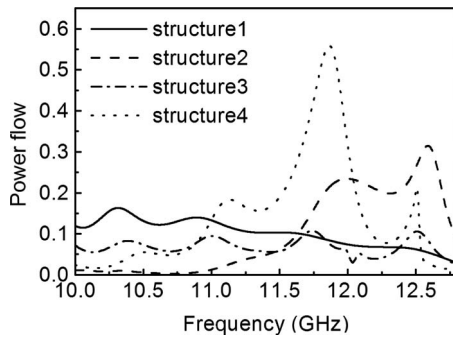
FIG. 2. Power flow versus frequency measured through boundary bnd0 for the four structures which are only the waveguide inside the PC (structure 1), the waveguide with the grating layers (structure 2), the waveguide with the modified surface layers (structure 3), and the waveguide with both the modified surface and the grating layers (structure 4).

is important to remind the reader that the main purpose of this paper is to present a structure that possesses a good beaming. High transmission of the channel and high directionality can be totally unrelated concepts; however, if the purpose is to achieve a very good beaming, the two components become equally important and having a high transmission together with a high directionality can assure a good beaming in our structure. We will first examine the transmission of the channel. Figure 2 displays the power flow versus the frequency for the four cases measured through a boundary (bnd0). The power flow is frequency dependent as it is clearly shown from Fig. 2. This figure shows that the transmission of the waveguide depends on the frequency and es-

pecially for the structures that grating and both grating and modified surface layers are added. Second, depending on the termination of the basic structure (structure 1), the transmission of the channel is very sensitive to what is at its ends or termination. Notice that for the case of structure 1, i.e., only the waveguide without modified surface and grating layers, the transmission for the whole range of frequencies is very low. However, when the grating and the modified surface layers are added (structure 4, dotted line in Fig. 2), the power flow is more than five times higher and reaches its maximum of 50% at the frequency of 11.85 GHz which corresponds to the beaming frequency.

To study the effect of the directionality, we normalize the power flow at the three boundaries (bnd1, bnd2, and bnd3) by the transmission through the waveguide (bnd0 in Fig. 1). Thus, we exclude the transmission through the channel and we get more information about the directionality of the beam. Figure 3 shows the power flow for the four cases at these three boundaries. In Fig. 3(a), the image of a diffraction pattern through an aperture is trivial and of course, the energy is diffracted in all directions which explains this power drop. For Fig. 3(b), the grating layer added to the photonic crystal waveguide in structure 2, although not designed to accommodate surface modes, does perturb the PC dispersion at the surface, just enough to support weakly coupling surface modes (with different dispersion than those on the modified surface layer). Therefore, for some frequencies, we observe a peak which corresponds to the excitation of these weak surface modes. For Fig. 3(d), the surface waves are best excited (large amplitude of fields at the surface) at 11.99 GHz in structure 3 (waveguide+modified surface layer); however, the beaming is observed at 11.85 GHz for structure 4 (waveguide+modified surface+grating layers).
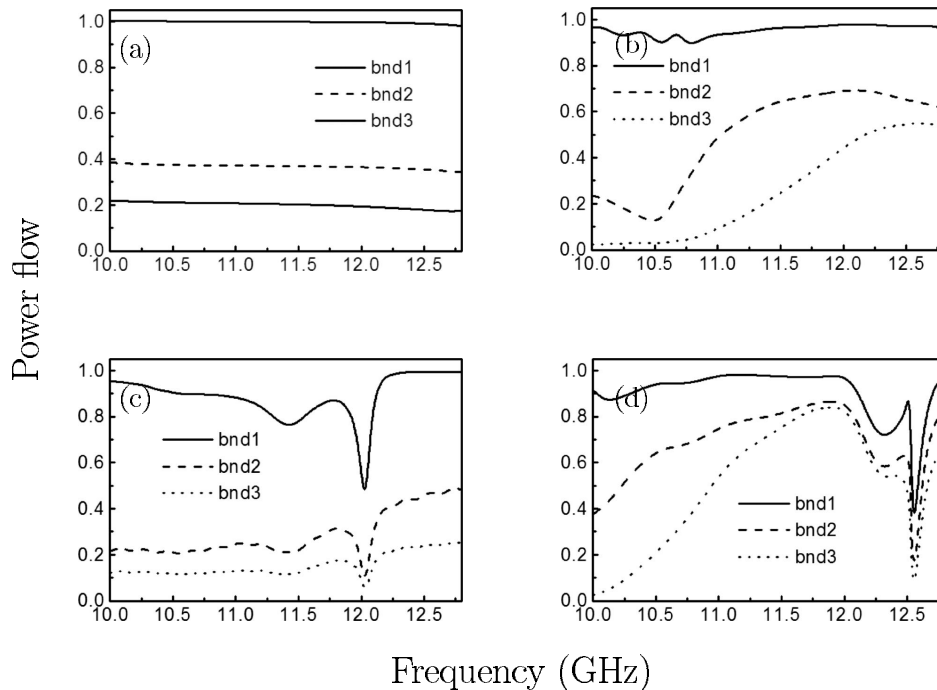


FIG. 3. Normalized power flow with respect to bnd0 versus frequency at the three different boundaries bnd1, bnd2, and bnd3 for (a) structure 1, (b) structure 2, (c) structure 3, and (d) structure 4.
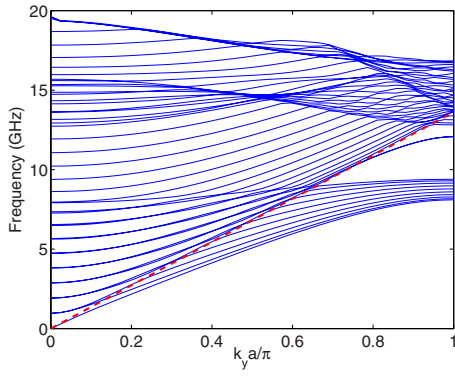
FIG. 4. (Color online) Band structure of the surface modified PC infinitely long in the lateral direction. The red dashed line shows the light line and the curve which is under the light line and in the middle of the band gap is the surface band.



FIG. 5. (Color online) A 2D plot of the strength of the electric field of structure 3 at (a) $f=11.97$ GHz and (b) $f=11.33$ GHz.

In fact by adding a layer of grating at the top of the modified surface, one does perturb the surface mode excitation frequency and shift it from 11.99 to 11.85 GHz. The dispersion relation for structure 3 (discussed later on in Fig. 4) shows that there are few frequencies for which we can excite surface modes, and the larger the parallel momentum, the larger the magnitude of the fields for the excited surface modes. For this structure, some of the frequencies happened to be 11.35 GHz (quite weak surface modes) and 11.99 GHz (strong surface modes). In order to get the beaming, the wavelength of the excited surface mode should correspond exactly to the lattice constant of the grating layer, which is $2a$. Therefore, the surface modes excited at 11.99 GHz in structure 3 couple to the outgoing beam and give rise to the beaming happening at 11.85 GHz. Notice that there is a drop of the power flow in Fig. 3(d) at 12.5 GHz. Indeed, the new setup of structure 4 does excite some surface waves at this frequency but because the condition to couple them to the outgoing waves is not fulfilled, most of this energy goes to the sides and a huge drop in the transmission is seen in Fig. 3(d). For all the cases, the transmission drops considerably when passing from bnd1 to bnd3, except for the fourth case [structure 4, see Fig. 3(d)], at the beaming frequency. For this case, and exactly at the frequency of 11.85 GHz, the power flow is at its maximum and it decreases by 10% when one measures it to bnd2 relative to bnd1. Therefore, from the end of the PC until bnd3, the intensity of the beam is almost the same (see the movie[23] that will be presented as a supplementary material) and the directionality is very good. Such result implies that the directionality of the beam depends strongly on the termination of the channel and when both modified surface and grating layers are at the end of the channel, both the transmission through the channel as well as the directionality are very good at a specific frequency, of course.

We already attribute the dips in the power flow observed close to 12 and 11.35 GHz in Fig. 3(c) to the excitation of the surface waves at the interfaces of the PC but let us examine those carefully by investigating the dispersion relation of the surface modes. The band structure of the modified surface PC, which extends to infinity in the lateral direction, is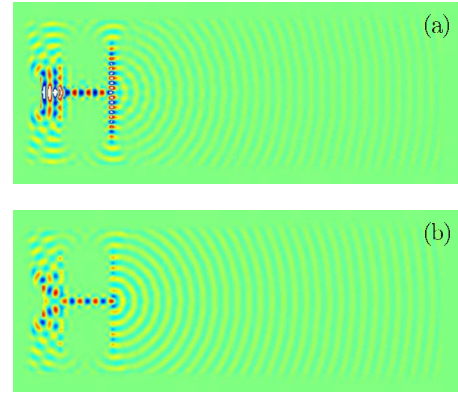 shown in Fig. 4, where a surface band can be seen inside the band gap and under the light line. Since the waves coming out from the PC waveguide tend to diffract in all directions, they have all $k_\parallel$ components. Thus, for any frequency in the range of the surface band, there exists some $k_\parallel$ that satisfies the dispersion relation of the surface band. So the surface wave excitation should be continuous over the spectrum for the infinite PC. However, in our study, the PC has a finite size with 21 rods in the lateral direction. The surface wave excitation in this case is discrete rather than continuous. This is because, at this finite and discrete surface layer, the possible values of $k_\parallel$ are discrete. In the first Brillouin zone, $k_\parallel$ can be $\frac{2\pi}{Na}m$, where $N=21$ is the total number of unit cells along the surface and $m$ is any integer between $-10$ and 10. From the dispersion curve, when $m=10$, the first surface mode is excited at $f=11.97$ GHz [Fig. 5(a)]; when $m=9$, the second surface mode is excited at $f=11.33$ GHz [Fig. 5(b)]. The first mode is expected to be the strongest since it has the largest $k_\parallel$, so the electromagnetic energy is most confined in the surface layer. However, in Fig. 5(b), in which $k_\parallel$ is smaller, the surface waves are not as strong as for the case of Fig. 5(a). When a surface wave is created, most of the energy coming from the channel does spread on the interface and very little goes to the forward direction. Consequently, the transmission outside the PC vanishes around these frequencies. So we see a strong dip when the first surface mode is excited and a shallower dip when the next surface mode is excited. When a grating layer is added to the PC with the modified surface layer (structure 4), the dispersion relation of the structure is modified and the transmission properties change drastically. The strong dip at around 12.5 GHz in Fig. 3(d) is due to the surface wave excitation at that frequency. All these features can be seen in the movie provided as supplementary material.

As it was mentioned earlier, these results are expected; thus, for structure 1, the structure transmits poorly and we did overcome this problem by changing the interface with a modified surface layer to enhance the transmission and with a grating layer to couple these excited surface modes to the outgoing one. We experimentally checked the transmission of structure 4 and the result is plotted in Fig. 6. A very good agreement is found between the simulation results shown as solid line and the experimental results shown as dashed line.
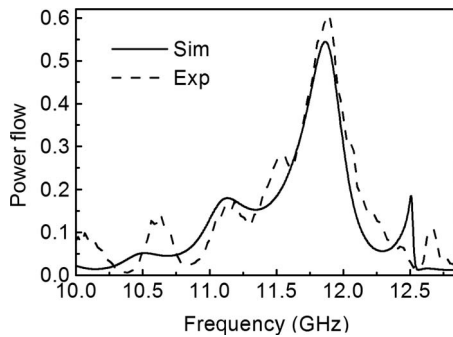
FIG. 6. Simulation and experimental power flows versus frequencies for structure 4, which possesses both the grating and the modified surface layers.

For both the simulation and the experiment, the beaming in the forward direction occurs at 11.85 GHz.

To show how the transmission of the channel (or waveguide) depends strongly on the channel termination, the fourth structure is slightly modified by taking away one grating at the middle of both grating layers. This modified structure will be referred to as structure 5. Figure 7 displays the simulation and the experimental results of the power flow for structure 5 in comparison with those of structure 4. First, the most striking change is the transmission enhancement of almost 20% at 11.85 GHz, by just removing only one grating in front of the channel. Second, a very strong transmission peak (more than 80%) is observed at 12.5 GHz making this structure a good candidate to have two strong transmissions at two different frequencies. It can be inferred that the back and forth reflection inside the waveguide is very sensitive to any small changes introduced into the structure. Consequently, it plays a major factor in determining the strength of the transmission, and therefore the quality of the beaming, if it is achieved together with a high directionality. The agreement between the experiment and the simulation is quite good, except at low frequency where the experimental results show some structure that can be attributed to the normalization procedures used in the experiment. To gain further insight on the consequences of the removed grating on the directionality, the normalized power flow for both cases
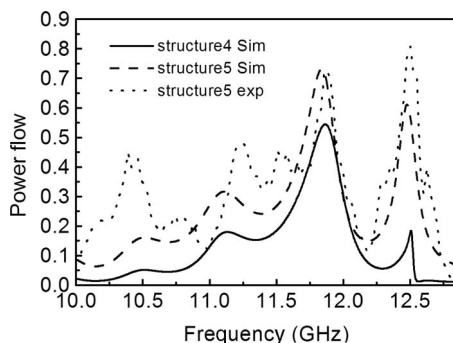


FIG. 7. Power flow versus frequency for structure 4 (simulation only) and structure 5 (simulation and experiment). Notice that structure 5 is similar to structure 4, except for the one grating missing in front at the end of the waveguide.
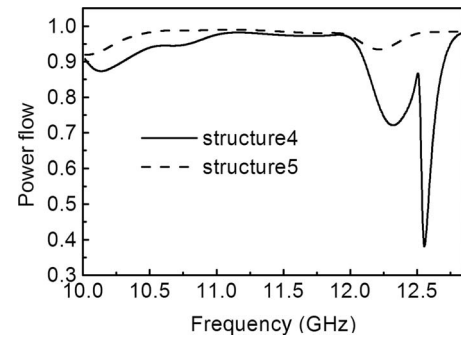


FIG. 8. Normalized power flow with respect to bnd0 of structures 4 and 5.

given by structures 4 and 5 is plotted in Fig. 8. Once more, the normalized power flow is derived by dividing the power flow at each boundary by the power flow inside the channel (bnd0). The power flow of structure 5 (dashed line) is more than 92% for almost all the frequencies compared to structure 4, in which a prominent drop of the transmission due to the excitation of the surface waves is observed around 12.54 GHz. Structure 5 is a good example of how the termination of the channel affects both the transmission of the channel and the directionality. Indeed, with just one grating removed, most of the energy in the channel is transmitted. Structures 4 and 5 are good examples of structures that possess good beaming resulting from the good coupling of the surface waves to the outgoing modes, contrary to a previous structure in which the transmission did not exceed 50%.[16]

One of the purposes of this paper is to fully understand the mechanism of beaming in the forward direction. As mentioned earlier, for the surface waves to couple to the continuum, a periodic grating modulation is necessary. The beaming is expected to occur when the grating period coincides with the wavelength of the surface waves. Fourier transform of the field at the interface where surface waves are excited can be used to precisely determine the wavelength of the surface waves. The surface waves are nothing but standing waves that propagate in both directions on the interface and, as expected, the Fourier transform of the electric field at the modified surface layer should show two peaks at $+k$ and $-k$. These two strongest peaks correspond to the excitation of the surface modes and occurs at the expected position ($\lambda = 22$ mm), which is exactly the lattice constant of the grating layers. The intensity of the peak is an indication of the strength of the excited surface waves at the modified surface layers.

To determine the impact of the modified surface and grating layers on the mechanism of the excitation of the surface waves as well as on the beaming and better understand the appearance of a second beaming in structure 5, Fourier analysis is used to derive the dispersion relation of the surface modes for the two cases (structures 3 5). Indeed, the dispersion relation was derived by analyzing the Fourier transform of the field at the modified surface layer and taking the wave vector of the highest peak found at each frequency. Figure 9 shows the dispersion relation as well as the high peak intensity for the third and fifth structures. The corre-
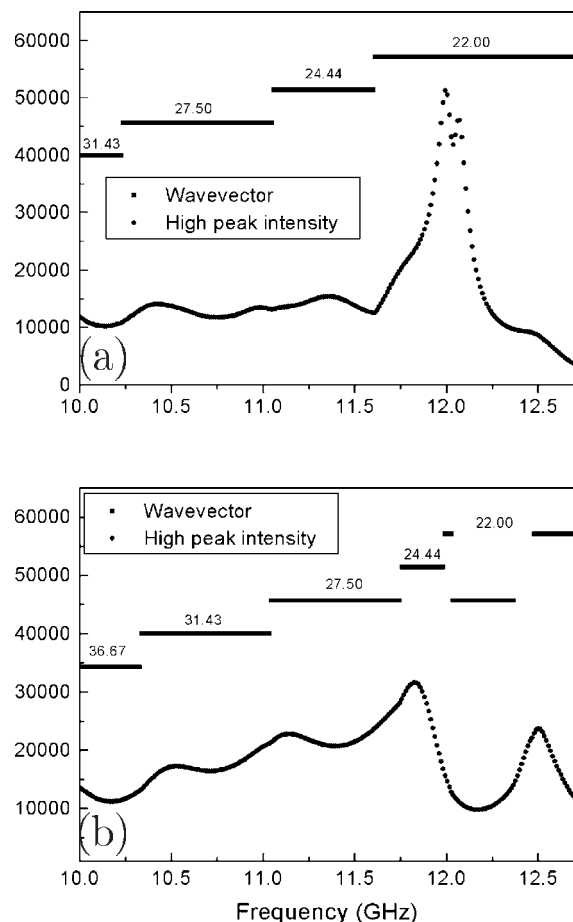
FIG. 9. Dispersion relation (wavevector versus frequency) and the high peak intensity versus the frequency for (a) structure 3, and (b) structure 5. The numbers at the top of each segment of the wave vector represents the corresponding wavelength in millimeters. To be able to put the two graphs, dispersion relation as well as the high peak intensity in the same graphs, the peak intensity is set 200 times higher than the real value.

sponding wavelength of the surface waves is given in millimeters and it is shown at the top of each wave vector segment. From Fig. 9(a), it can be seen that the surface waves excited at the modified surface layers correspond to a wavelength of $\lambda = 22$ mm and appear at a frequency of 11.99 GHz. At this frequency, the intensity of the peak is the highest, showing very strong surface modes, when it is compared to other surface modes excited at different frequencies. Notice that the wavelength of the surface waves at the first beaming frequency for structure 5 is $\lambda = 24.44$ mm, which deviates from $\lambda = 22$ mm mostly due to the presence of the grating layer that disturbs and changes the environment for the surface waves. The change of the dispersion relation from structure 3 to structure 5 is clearly seen in Fig. 9(b). By adding the grating layer at the top of the modified surface one, the whole dispersion relation seems to be lowered in terms of wave vector [Figs. 9(a) and 9(b)]. From Fig. 9(b), it can be seen that the high peak intensity of the surface waves at the first beaming frequency, 11.85 GHz, is stronger compared to the one at 12.5 GHz. In conclusion, Fourier analysis did help us understand the occurrence of two beamings for structure 5 and gave us an idea about the strength of the surface waves excited and involved in the beaming phenomena.

For further insight on the strength of the field at both beaming and nonbeaming frequencies, we plot the experimental and the simulation results for structure 4 in Fig. 10. The figure is a two dimentional (2D) plot of the strength of the electric field for both experimental [Figs. 10(a) and 10(c)] and simulation results [Figs. 10(b) and 10(d)]. At the beaming frequency (i.e., 11.85 GHz), structure 4 generates a very nice beaming that goes further away from the PC with noticeable intensity. However, at the nonbeaming frequency (i.e., 12.47 GHz), the beaming effect disappears, and both experimental and simulation results show a nonpronounced field outside the PC that splits into two directions and vanishes afterward. For more details on the field strength for the whole range of frequency, refer to the movie that is added as a supplementary material with the paper.

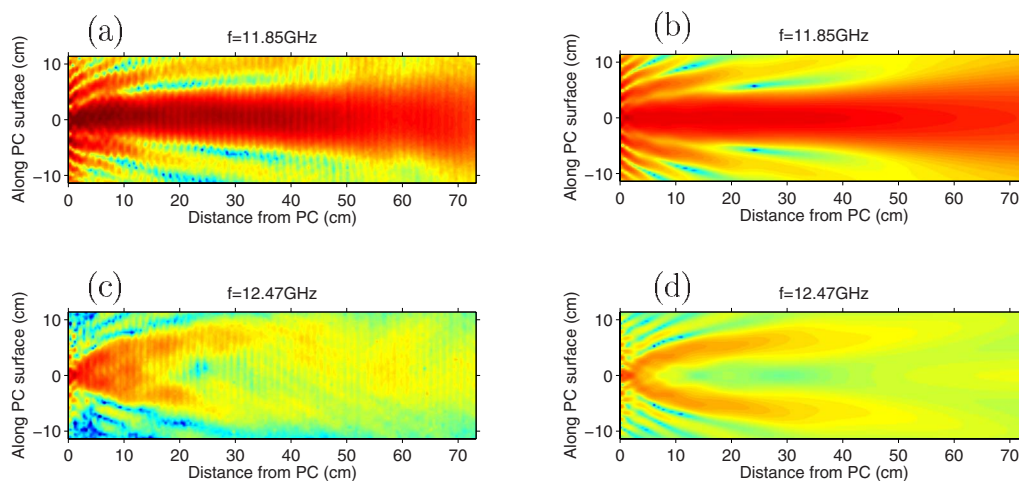In Fig. 11, we examine structure 5 as we did with struc-



FIG. 10. (Color online) A 2D plot of the strength of the outgoing electric field for the case of structure 4. (a) and (b) are the experimental and the simulation results, respectively, at frequency $f = 11.85$ GHz. (c) and (d) are the experimental and the simulation results, respectively, at frequency $f = 12.47$ GHz.
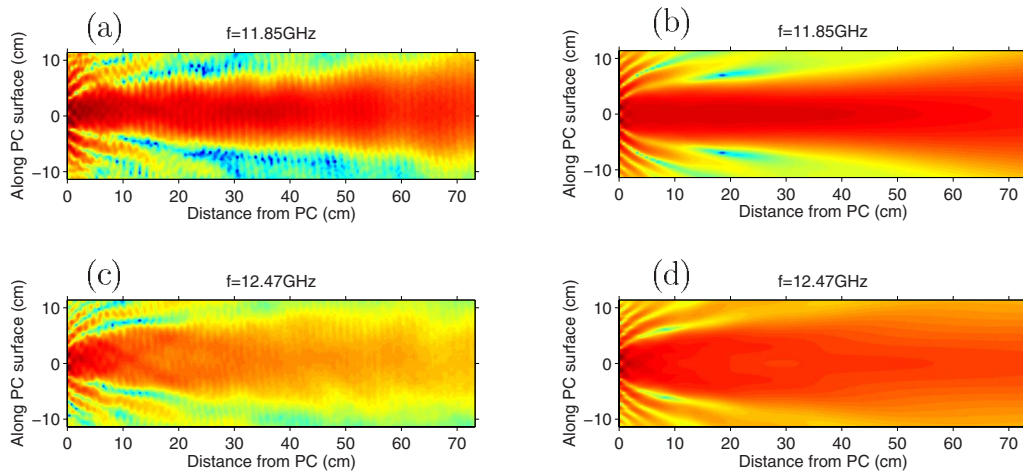
FIG. 11. (Color online) A 2D plot of the strength of the outgoing electric field for the case of structure 5. (a) and (b) are the experimental and the simulation results, respectively, at frequency $f=11.85$ GHz. (c) and (d) are the experimental and the simulation results, respectively, at frequency $f=12.47$ GHz.

ture 4 in Fig. 10. For this structure, the two chosen frequencies are both beaming frequencies. As shown in both the experimental and the simulation results the beaming at 11.85 GHz for this structure is more pronounced than that of structures 4 (Fig. 10). For the frequency of 12.47 GHz the field strength shows a second beaming as the power flow results given in Fig. 8 have predicted its existence. Therefore, a small change in the geometry of the structure results in a very interesting property, namely an increase of 20% for the beaming at the frequency of 11.85 GHz and the appearance of a second beaming at 11.47 GHz. Once again, the agreement between experiment and simulation is quite good.

The above-mentioned results are also presented in an animation that displays the distribution of the electric field for the five structures (structures 1–5) in five parallel panels. The movie is generated for 800 frequencies ranging from 10 to 13 GHz. For all the results displayed in the movie, the incident beam comes first from an air part, passes through the PC, and ends in a second air part (see Fig. 1). In order to observe the directionality, the height of the second air part is chosen to be five times higher than the PC's height. Some frames for the different cases of the animation have been plotted in Fig. 12 for frequencies that are of interest. The frequency of the source was selected to be in the gap. Therefore, nothing propagates inside the PC except in the waveguide in which strong localization of the field is shown in the channel along the propagation direction and decays in the lateral direction. For all the frequencies of the incident beam, the aperture is smaller than the wavelength of the incident beam and the aperture transmits very poorly and diffracts light in all directions. This is clearly seen in the case of the first panel, which displays the distribution of the electric field for the waveguide PC without any extra layers. For this case, the surface of the PC does not support any surface waves. For the other cases in which other layers are added, the transmission is no longer the same. The reason is the extra layers with different geometrical parameters added to the PC that disturb the dispersion and enable surface waves to be excited. Since the surface modes lie below the light line, they

cannot be excited by an incident plane wave. The presence of extra layers helps the excited surface waves to couple to the free propagating EM waves. Even though the grating layer in the second panel of the movie does not fulfill completely the transformation of the wave vector, we could see some enhancement of the wave at the interface around 11.90 and 12.45 GHz. For the second panel (structure 2), the transmission is suppressed until the frequency of 11 GHz, after which
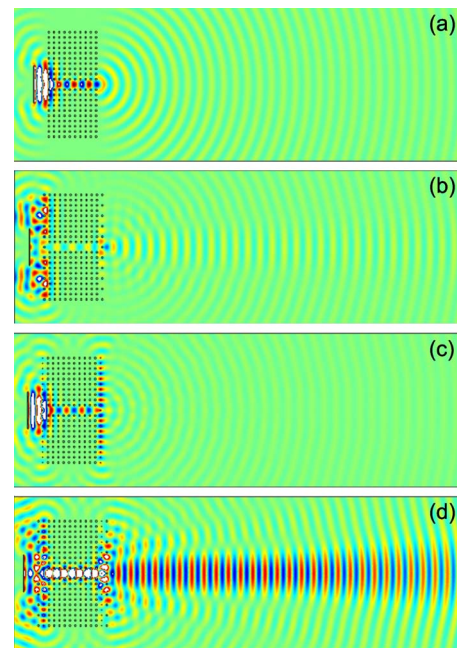


FIG. 12. (Color online) Frames picked from the movie. (a) shows the electric field distribution of structure 1 (only waveguide) at frequency $f=11.97$ GHz, (b) shows the electric field distribution of structure 2 (waveguide and grating) at frequency $f=11.85$ GHz, (c) shows the electric field distribution of structure 3 (waveguide and modified surface layers) at frequency $f=11.97$ GHz, and (d) shows the electric field distribution of structure 4 (waveguide with modified surface and grating layers) at frequency $f=11.85$ GHz.

a beam in the forward direction propagates and splits later into two beams. The case of the third panel (structure 3) shows a real surface wave excitation at different frequencies but the most enhanced one is the surface wave excited at 11.99 GHz, in which we see the typical profile of standing waves propagating along the parallel direction to the interfaces and decaying in the perpendicular one. The intensity of the enhanced surface waves at this specific frequency exceeds the intensity of the field in the channel. Panel 4 displays the electric field for structure 4 and shows the beaming that begins at 10.90 GHz and reaches its maximum at 11.85 GHz. Almost all the excited surface waves transform their energy to the outgoing beam. Panel 5 shows the two beaming phenomena at 11.85 and 12.5 GHz for structure 5. The movie is a real time demonstration of what we discussed earlier about the excitation of the surface modes, the energy that gets lost and goes to the sides, and the nice buildup of the beaming in the forward direction.

In conclusion, we studied the effect of the modified surface and the grating layers on the beaming properties of our PC. Our experimental and simulation results show that there are two factors for the beaming phenomenon: the transmission of the waveguide and the directionality of the beam. The termination of the waveguide, which is dictated by the back and forth transmission in the waveguide, has an important effect on the transmission and the directionality. Indeed, our results demonstrate ways to improve the beaming in the forward direction. In fact, a small modification in the grating layer gives rise to an increase of 20% in the intensity of the field and opens up another frequency region for a second beaming. Furthermore, the derived dispersion relation for the surface modes emphasizes on the impact and the effect of the geometrical parameters, namely, the modified surface and grating layers.

[1] T. W. Ebbesen, H. J. Lezec, H. F. Ghaemi, T. Thio, and P. A. Wolff, Nature (London) **391**, 667 (1998).

[2] L. Martín-Moreno, F. J. García-Vidal, H. J. Lezec, K. M. Pellerin, T. Thio, J. B. Pendry, and T. W. Ebbesen, Phys. Rev. Lett. **86**, 1114 (2001).

[3] L. Martín-Moreno, F. J. García-Vidal, H. J. Lezec, A. Degiron, and T. W. Ebbesen, Phys. Rev. Lett. **90**, 167401 (2003).

[4] H. J. Lezec, A. Degiron, E. Devaux, R. A. Linke, L. Martín-Moreno, F. J. García-Vidal, and T. W. Ebbesen, Science **297**, 820 (2002).

[5] J. R. Sambles, Nature (London) **391**, 641 (1998).

[6] S. I. Bozhevolnyi, J. Erland, K. Leosson, P. M. W. Skovgaard, and J. M. Hvam, Phys. Rev. Lett. **86**, 3008 (2001).

[7] For a recent review, see C. Genet and T. W. Ebbesen, Nature (London) **445**, 39 (2007).

[8] R. D. Meade, K. D. Brommer, A. M. Rappe, and J. D. Joannopoulos, Phys. Rev. B **44**, 10961 (1991).

[9] W. M. Robertson, G. Arjavalingam, R. D. Meade, K. D. Brommer, A. M. Rappe, and J. D. Joannopoulos, Opt. Lett. **18**, 528 (1993).

[10] S. Xiao, M. Qiu, Z. Ruan, and S. He, Appl. Phys. Lett. **85**, 4269 (2004).

[11] R. Moussa, Th. Koschny, and C. M. Soukoulis, Phys. Rev. B **74**, 115111 (2006).

[12] B. Wang, W. Dai, A. Fang, L. Zhang, G. Tuttle, Th. Koschny, and C. M. Soukoulis, Phys. Rev. B **74**, 195104 (2006).

[13] P. Kramper, M. Agio, C. M. Soukoulis, A. Birner, F. Muller, R. B. Wehrspohn, U. Gosele, and V. Sandoghdar, Phys. Rev. Lett. **92**, 113903 (2004).

[14] E. Moreno, L. Martín-Moreno, and F. J. García-Vidal, Photonics Nanostruct. Fundam. Appl. **2**, 97 (2004).

[15] E. Moreno, F. J. García-Vidal, and L. Martín-Moreno, Phys. Rev. B **69**, 121402(R) (2004).

[16] I. Bulu, H. Caglayan, and E. Ozbay, Opt. Lett. **30**, 3078 (2005).

[17] S. K. Morrision and Y. S. Kivshar, Appl. Phys. Lett. **86**, 081110 (2005).

[18] A. I. Rahachou and I. V. Zozoulenko, Phys. Rev. B **72**, 155117 (2005).

[19] W. Śmigaj, Phys. Rev. B **75**, 205430 (2007).

[20] J. Bauer and S. John, Appl. Phys. Lett. **90**, 261111 (2007).

[21] http://www.comsol. com/

[22] J.-P. Berenger, J. Comput. Phys. **114**, 185 (1994); IEEE Trans. Antennas Propag. **44**, 110 (1996).

[23] See EPAPS Document No. E-PRBMDO-76-071747 for an animation that displays the distribution of the electric field for the five structures (structures 1–5) in five parallel panels. For more information on EPAPS, see http://www.aip.org/pubservs/epaps.html.